Wire-width dependence of the LO-phonon splitting and photoluminescence energy in $ZnSe/Cd_{0.35}Zn_{0.65}Se$ quantum wires

G. Lermann, T. Bischof, A. Materny, and W. Kiefer*
Institut für Physikalische Chemie der Universität Würzburg, Am Hubland, D-97074 Würzburg, Federal Republic of Germany

T. Kümmell, G. Bacher, A. Forchel, and G. Landwehr
Physikalisches Institut, Universität Würzburg, Am Hubland, D-97074 Würzburg, Federal Republic of Germany
(Received 3 April 1997)

$Cd_xZn_{1-x}Se/ZnSe$ quantum wires with lateral widths down to 13 nm were fabricated by electron-beam lithography and wet chemical etching. In order to study the wire-width dependence of both the LO-phonon splitting between the barrier and the wire regions and the emission energy, micro resonance Raman spectroscopy and photoluminescence (PL) measurements have been performed. Reducing the wire width down to about 30 nm, we found an increasing splitting between the ZnSe phonon of the barrier layers and the ZnSe-like phonon of the $Cd_xZn_{1-x}Se$ wire regions as well as an increasing redshift of the PL energy. This behavior is due to the strain relaxation of the deeply etched, biaxially strained wires. By calculating the size dependence of the strain distribution and the LO-phonon wave numbers, good agreement between experiment and theory is obtained. Decreasing the wire size further down to the sub-20-nm range, the LO splitting is found to be almost independent of the wire width, indicating no further change of the strain relaxation. In this range, the PL spectrum shows a blueshift with decreasing wire size due to lateral carrier confinement. [S0163-1829(97)00436-0]

I. INTRODUCTION

Recently, quantum wires of several II-VI semiconductors have attracted considerable attention.[1–4] This is due to the restriction of the vibrational and electronic (vibronic) system to only one dimension. New physical phenomena are expected, which strongly depend on the width of the wires, for example, a blueshift of the band gap due to lateral confinement of electrons and holes.[5,6] Up to now, only a little information on II-VI semiconductor quantum wires can be found in the literature, mainly reporting on the dependence of the luminescence on the wire width.[4,7]

As confinement effects seem to occur only for wires that are thinner than about 40 nm, great efforts have been made regarding refined etching process.[5,6] Wire sizes down to 13 nm have been achieved.[6] Considering the photoluminescence (PL) spectra for decreasing wire widths, an increasing redshift of the PL energy has been detected as long as confinement effects could be neglected.[5,6] This can be explained as a result of strain and strain relaxation, which directly influences the band gap of the nanostructures.[8,9] For a further decrease of the wire width, an additional blueshift of the PL energy occurs due to lateral confinement of electrons and holes.

In this paper we report experimental and theoretical results concerning the correlation between the wire width dependence of the LO-phonon frequency and the band gap of the quantum-well layer in $ZnSe/Cd_xZn_{1-x}Se$ semiconductor nanostructures. Micro-Raman measurements and PL experiments have been performed. A strong wire width dependence of the PL energy and of the ZnSe-like LO-phonon wave-number position for wires thinner than 100 nm has been found. This behavior is explained by strain relaxation in the $Cd_xZn_{1-x}Se$ layer in the wire.

II. EXPERIMENT

The quantum-wire sample under investigation is shown schematically in Fig. 1. On a GaAs substrate a GaAs buffer layer, a ZnS_xSe_{1-x} buffer layer, and subsequently a $ZnSe/Cd_xZn_{1-x}Se$ quantum well were grown with a molecular-beam epitaxy Riber system. The ZnS_xSe_{1-x} buffer layer is 620 nm thick with a sulphur content of 6% in

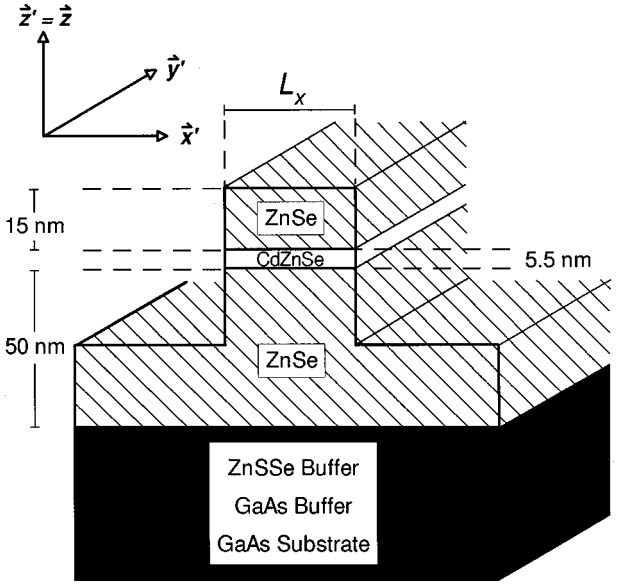

FIG. 1. Schematic representation of the quantum wires under investigation.

order to get lattice matching between the GaAs and ZnS_xSe_{1-x} layer. The bottom barrier layer is ZnSe and has a thickness of 50 nm. The quantum-well layer of thickness 5.5 nm consists of $Cd_xZn_{1-x}Se$ with a concentration of 35% cadmium. As a cap layer 15 nm of ZnSe is used. The cadmium concentration as well as the thickness of the layers have been verified by x-ray diffraction.

To obtain wires of widths L_x down to 13 nm these quantum wells were patterned by electron-beam lithography and wet chemical etching, as described in detail in Refs. 5 and 6. The wires are oriented in the (110) direction. For such a structure the strain between different layers plays a very important role. While the ZnSe layer is almost lattice matched to the $ZnS_{0.06}Se_{0.94}$ buffer, the quantum-well layer is strained due to the Cd that is incorporated into the ZnSe lattice. The lattice constant of CdSe ($a=6.052$ Å) is larger than that of ZnSe ($a=5.668$ Å).[10] In order to avoid lattice relaxation in our samples the thickness of the quantum-well layer was kept small.

The samples used in our experiments consisted of several patterned areas of $70\times70\ \mu m^2$, each containing wires of well-defined width separated by several 100 μm from each other. Therefore, within the focal area of the laser, which is about $0.8\ \mu m^2$ for the Raman measurements and about $50^2\ \mu m^2$ in the case of the PL measurements, the widths as well as the compositions of the wires were always the same. Different wire widths were investigated by focusing the laser beam into the different patterned areas of the sample.

In order to obtain laterally resolved Raman data from the samples a micro-Raman setup was used. The Raman microscope has been described in detail elsewhere.[11] The micro-Raman spectra were recorded using an excitation wavelength of 472.7 nm of an argon-ion laser (Spectra Physics Model 166). An adaption lens focused the Raman light onto the entrance slit of a Spex 1404 double spectrometer equipped with a charge coupled device (CCD) camera system (Photometrics model 9000). The sample was placed in a closed cycle cryostat (CTI Cryogenics), which enabled us to vary the temperature of the sample from room temperature down to about 9 K. The accuracy of the chosen temperature was about ±5 K. The working distance of the microscope objective was 4.2 mm. Therefore, we had to use a very thin (1-mm) window for the cryostat and the sample surface had to be placed very close to the window.

In order to avoid sample heating, the measurements were performed using a laser power of only about 5 mW. Micro-Raman spectra were recorded by applying the scanning multichannel technique.[12] The spectral resolution was about $2\ cm^{-1}$.

In addition to the Raman experiments, low-temperature (2 K) PL measurements on the same wire structures were performed. The 363.8-nm line of an Ar^+ laser was used for the excitation of the sample with a power of 5 mW. The PL was dispersed by a 0.32-m monochromator and detected with a CCD camera.

III. THEORETICAL CONSIDERATIONS

The consequence of the presence of strain in semiconductor heterostructures was the subject of many experimental and theoretical investigations.[13–16] Therefore, the influence of strain on the phonon frequency is well known from the literature. But to our knowledge no theoretical considerations of the influence of strain and strain relaxation in semiconductor quantum wires including the contribution of shear strain components on the LO-phonon wave-number positions have been published until now. Our theoretical considerations are based on the calculation of the strain components as a function of the coordinates of a strain relaxed quantum wire.

First, we consider a two-dimensional field (mesa) of our sample. The bottom ZnSe layer (50 nm) and the top ZnSe layer (15 nm) are very thick compared to the quantum-well layer (5.5 nm $Cd_{0.35}Zn_{0.65}Se$) in between. Therefore, we assume that the $Cd_{0.35}Zn_{0.65}Se$ lattice has the same in-plane lattice constant as the ZnSe lattice. This means that the $Cd_{0.35}Zn_{0.65}Se$ quantum-well layer is under biaxial compressive strain.

In the case of a structured semiconductor, for example, quantum wires, strain relaxation occurs at the edge of the wires. For the calculation of this strain relaxation some definitions have to be made. The Cartesian crystal coordinates are in the (100), (010), and (001) directions of the crystal lattice and are denoted by ($\mathbf{x}$,$\mathbf{y}$,$\mathbf{z}$). The growth direction is $\mathbf{z}$. The Cartesian wire coordinates are in the (110), (1$\bar{1}$0), and (001) directions and are denoted by ($\mathbf{x}'$,$\mathbf{y}'$,$\mathbf{z}'$). The wires are oriented parallel to the (110) $\mathbf{y}'$ direction. The width of the wire is in the $\mathbf{x}'$ direction and the height is in the $\mathbf{z}'=\mathbf{z}$ direction (see Fig. 1). For convenience, we will use primed symbols in the wire coordinates instead of primed indices in the subscripts, i.e., we will use ϵ'_{yy} for $\epsilon_{y'y'}$. Since the dimension of the wire in the $\mathbf{y}'$ direction is large, ϵ'_{yy} is constant and is determined by the misfit between the ZnSe and $Cd_{0.35}Zn_{0.65}Se$ layers. Therefore, the problem is reduced to the $\mathbf{x}'$-$\mathbf{z}'$ plane.

A. Calculation of the strain relaxation

In strained quantum wells, the in-plane strain is described by the relative lattice mismatch of the (unstrained) barrier and well material:

$$\epsilon_{xx}=\epsilon_{yy}=(a_{\mathrm{barr}}-a_{\mathrm{well}})/a_{\mathrm{well}}. \tag{1}$$

In the $Cd_xZn_{1-x}Se$/ZnSe material system the lattice constant of $Cd_xZn_{1-x}Se$ is larger than the lattice constant of ZnSe ($a_{\mathrm{well}}>a_{\mathrm{barr}}$), leading to a compressive (negative) in-plane strain. This compressive strain is counterbalanced by an increased lattice constant, i.e., a tensile (positive) strain, in the growth direction:

$$\epsilon_{zz}=-\frac{c_{13}+c_{23}}{c_{33}}\cdot\epsilon_{xx}. \tag{2}$$

The c_{ij} can easily be evaluated from the elastic constants because $c_{13}=c_{23}=c_{12}$ and $c_{33}=c_{44}$. In the $Cd_{0.35}Zn_{0.65}Se$/ZnSe system, ϵ_{xx} and $\epsilon_{yy}=-0.0229$ and $\epsilon_{zz}=0.0286$. Thus we have a biaxially strained layer with all shear strain components $\epsilon_{xy}=\epsilon_{xz}=\epsilon_{yz}=0$.

For an as-etched wire structure, there are no restrictions at the wire sidewalls, causing a partial lattice relaxation. To calculate this relaxation, we defined a grid upon the cross section of the wire and minimized the strain energy for each

grid point with respect to its nearest neighbors. Similar investigations have been made in Refs. 17 and 18, using a finite-element method, applied to strain effects in as-etched and overgrown wires, respectively. As expected, $\epsilon'_{xx}, \epsilon'_{zz}, \epsilon'_{xz}$ are functions of the wire cross section coordinates $\mathbf{x}'$ and $\mathbf{z}'$. In principle, ϵ'_{xx} and ϵ'_{zz} are decreasing at the wire sidewalls and for narrow wires even in the wire center. In contrast to two-dimensional (2D) material, the shear strain component ϵ'_{xz} is not zero in particular at the wire edges.

B. Shift of the LO phonon in strained quantum wires

Biaxial compressive strain shifts the LO phonon to higher frequencies.[15] The strain-induced shift $\Delta\tilde{\nu}$ of a phonon is determined by the solution of the following secular equation derived by Anastassakis:[13]

$$\begin{vmatrix} m_{11}-\lambda & m_{12} & m_{13} \\ m_{21} & m_{22}-\lambda & m_{23} \\ m_{31} & m_{32} & m_{33}-\lambda \end{vmatrix} = 0, \tag{3a}$$

where

$$\begin{aligned} m_{11} &= K_{11}\epsilon_{xx} + K_{12}(\epsilon_{yy}+\epsilon_{zz}), \\ m_{12} &= 2K_{44}\epsilon_{xy}, \\ m_{13} &= 2K_{44}\epsilon_{xz}, \\ m_{21} &= 2K_{44}\epsilon_{yx}, \\ m_{22} &= K_{11}\epsilon_{yy} + K_{12}(\epsilon_{zz}+\epsilon_{xx}), \\ m_{23} &= 2K_{44}\epsilon_{yz}, \\ m_{31} &= 2K_{44}\epsilon_{zx}, \\ m_{32} &= 2K_{44}\epsilon_{zy}, \\ m_{33} &= K_{11}\epsilon_{zz} + K_{12}(\epsilon_{xx}+\epsilon_{yy}). \end{aligned} \tag{3b}$$

Here K_{11}, K_{12}, and K_{44} are the phonon deformation potentials and the ϵ_{ij} are the strain components. The eigenvalues

$$\lambda_i = \frac{2}{\tilde{\nu}_0}\Delta\tilde{\nu}_i, \tag{4}$$

where $\tilde{\nu}_0$ is the Raman wave number of the bulk material and the $\Delta\tilde{\nu}_i$ are the shifts of the LO phonons with respect to the wave-number position in unstrained material. We use the phonon deformation potentials measured by Cerdeira *et al.*[14] Since there are no phonon deformation potentials known for CdSe, we use the ZnSe phonon deformation potentials for the $Cd_{0.35}Zn_{0.65}Se$ layer as well.

In order to solve the secular equation we have to transform the strain components into crystal coordinates. In Sec. III A the strain components were given referring to wire coordinates. The strains in crystal coordinates are calculated as

$$\epsilon = \begin{pmatrix} \frac{1}{2}(\epsilon'_{xx}+\epsilon'_{yy})+\epsilon'_{xy} & -\frac{1}{2}(\epsilon'_{xx}-\epsilon'_{yy}) & \frac{1}{\sqrt{2}}(\epsilon'_{xz}+\epsilon'_{yz}) \\ -\frac{1}{2}(\epsilon'_{xx}-\epsilon'_{yy}) & \frac{1}{2}(\epsilon'_{xx}+\epsilon'_{yy})-\epsilon'_{xy} & -\frac{1}{\sqrt{2}}(\epsilon'_{xz}-\epsilon'_{yz}) \\ \frac{1}{\sqrt{2}}(\epsilon'_{xz}+\epsilon'_{yz}) & -\frac{1}{\sqrt{2}}(\epsilon'_{xz}-\epsilon'_{yz}) & \epsilon'_{zz} \end{pmatrix}. \tag{5}$$

As mentioned above, we neglect strain relaxations along the $\mathbf{y}'$ direction (wire length) and therefore consider only the $\mathbf{x}'$-$\mathbf{z}'$ plane. With $\epsilon'_{yz}=\epsilon'_{xy}=0$ Eq. (5) can be reduced to

$$\epsilon = \begin{pmatrix} \frac{1}{2}(\epsilon'_{xx}+\epsilon'_{yy}) & -\frac{1}{2}(\epsilon'_{xx}-\epsilon'_{yy}) & \frac{1}{\sqrt{2}}\epsilon'_{xz} \\ -\frac{1}{2}(\epsilon'_{xx}-\epsilon'_{yy}) & \frac{1}{2}(\epsilon'_{xx}+\epsilon'_{yy}) & -\frac{1}{\sqrt{2}}\epsilon'_{xz} \\ \frac{1}{\sqrt{2}}\epsilon'_{xz} & -\frac{1}{\sqrt{2}}\epsilon'_{xz} & \epsilon'_{zz} \end{pmatrix}. \tag{6}$$

Using these strain components we are able to solve the secular equation (3a). From this we obtain the eigenvalues

$$\lambda_1 = K_{11}\epsilon_{xx} + K_{12}(\epsilon_{xx}+\epsilon_{zz}) + 2K_{44}\epsilon_{xy}, \tag{7}$$

$$\lambda_{2,3} = \tfrac{1}{2}\{K_{11}(\epsilon_{xx}+\epsilon_{zz}) + K_{12}(3\epsilon_{xx}+\epsilon_{zz}) - 2K_{44}\epsilon_{xy} \mp \sqrt{[(K_{11}-K_{12})(\epsilon_{xx}-\epsilon_{zz}) - 2K_{44}\epsilon_{xy}]^2 + 2(4K_{44}\epsilon_{xz})^2}\},$$

and the eigenvectors

$$\boldsymbol{\mu}_1=\begin{pmatrix}1\\1\\0\end{pmatrix},\quad \boldsymbol{\mu}_{2,3}=\begin{pmatrix}\dfrac{x\mp y}{v\mp w}\\ -\dfrac{x\mp y}{v\mp w}\\1\end{pmatrix}, \tag{8a}$$

with

$$x=\epsilon_{xy}[(K_{11}-K_{12})(\epsilon_{xx}-\epsilon_{zz})-2K_{44}\epsilon_{xy}]-4K_{44}\epsilon_{xz}^2,$$
$$y=\epsilon_{xy}\sqrt{[(K_{11}-K_{12})(\epsilon_{xx}-\epsilon_{zz})-2K_{44}\epsilon_{xy}]^2-32(K_{44}\epsilon_{xz})^2}, \tag{8b}$$
$$v=\epsilon_{xz}[(K_{11}-K_{12})(\epsilon_{xx}-\epsilon_{zz})+6K_{44}\epsilon_{xy}],$$
$$w=-\epsilon_{xz}\sqrt{[(K_{11}-K_{12})(\epsilon_{xx}-\epsilon_{zz})-2K_{44}\epsilon_{xy}]^4-32(K_{44}\epsilon_{zz})^2}.$$

In the backscattering geometry ($\mathbf{k}\|\mathbf{z}$), $\Delta\tilde{\nu}$ is determined by the eigenvalue belonging to the eigenvector (0,0,1) in crystal coordinates. In our case we have to transform the vector (0,0,1) into wire coordinates to obtain the coefficients that yield the contribution of each eigenvalue of the wire system. These coefficients, multiplied by the respective eigenvalues, provide the shift of the LO phonon $\Delta\tilde{\nu}$ observed in backscattering geometry:

$$\Delta\tilde{\nu}=\frac{\tilde{\nu}_0}{8(wx-vy)|v+w||v-w|}\{(v-w)\sqrt{(v-w)^2+2(x-y)^2}\sqrt{(v+w)^2}(x+y)\times[K_{11}(\epsilon_{xx}+\epsilon_{zz})+K_{12}(3\epsilon_{xx}+\epsilon_{zz})$$
$$-2K_{44}\epsilon_{xy}-\sqrt{[(K_{11}-K_{12})(\epsilon_{xx}-\epsilon_{zz})-2K_{44}\epsilon_{xy}]^2+32(K_{44}\epsilon_{xz})^2}]-(v+w)\sqrt{(v+w)^2+2(x+y)^2}\sqrt{(v-w)^2}$$
$$\times(x-y)\times[K_{11}(\epsilon_{xx}+\epsilon_{zz})+K_{12}(3\epsilon_{xx}+\epsilon_{zz})-2K_{44}\epsilon_{xy}+\sqrt{[(K_{11}-K_{12})(\epsilon_{xx}-\epsilon_{zz})-2K_{44}\epsilon_{xy}]^2+32(K_{44}\epsilon_{xz})^2}]\}. \tag{9}$$

Due to strain relaxation at the edge of the wire the strain is a function of $\mathbf{x}'$ and $\mathbf{z}'$. In Sec. III A the lattice relaxation has been calculated characterizing every lattice cell of the wire as one particular point. Considering one defined wire width, the strain relaxation as a function of x' and z' is characteristic for this wire width. Therefore, the calculated LO-phonon wave number as a function of x' and z' for one particular wire width is also a characteristic function for the considered wire width.

In Fig. 2 the calculated LO-phonon wave number is plotted as a function of the coordinates of the wire cross section ($\mathbf{x}'$-$\mathbf{z}'$ plane) for a 40-nm-wide quantum wire. The LO-phonon wave number in the bottom and top ZnSe layers of the wire is equal to the bulk phonon wave number of 257 cm^{-1}. In the $Cd_{0.35}Zn_{0.65}Se$ quantum-well layer the LO phonon is shifted to higher wave numbers compared to the bulk $Cd_{0.35}Zn_{0.65}Se$ phonon position[19] at 245 cm^{-1}. Due to the strain relaxation at the edge of the wire the strain-induced shift of the LO phonon of the quantum wire is higher in the center than at the edge of the wire.

In Fig. 3 the wave number of the LO phonon in the middle layer of the $Cd_xZn_{1-x}Se$ wire as well as in a mesa (2D) field is plotted as a function of the normalized wire width. Due to the boundary conditions in the theoretical model the wave-number position of the LO phonon at the edge is the same for each wire width. In the middle of the wire the strain relaxation increases for decreasing wire width. In wires 50 or 40 nm wide a shift of about 1 cm^{-1} with respect to the two-dimensional mesa is calculated. For a 20- and a 15-nm wire the shift is about 2 and 2.5 cm^{-1}, respectively.

IV. EXPERIMENTAL RESULTS

A. Raman scattering

Raman spectra were taken of different sample areas with well-defined wire widths. The micro-Raman setup enabled us to excite spectra only from a small spot and no overlap

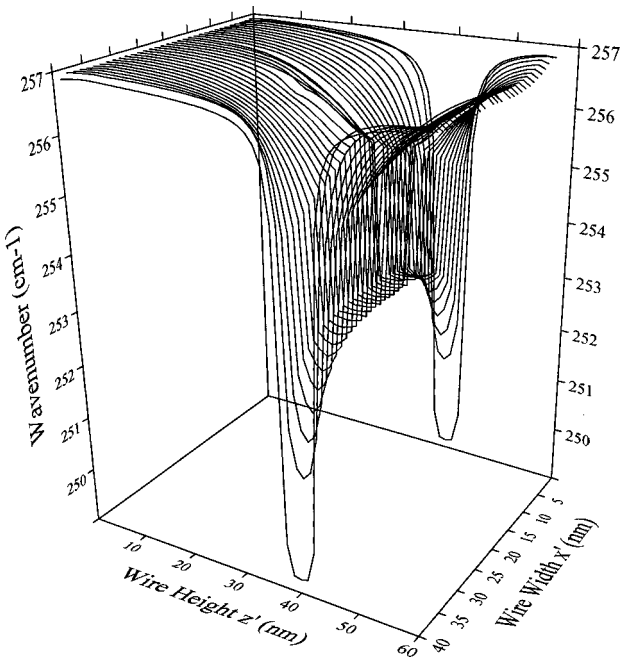

FIG. 2. Theoretical LO-phonon wave-number positions obtained for 40-nm $Cd_xZn_{1-x}Se$/ZnSe wires as a function of the coordinates spanning the wire cross section.

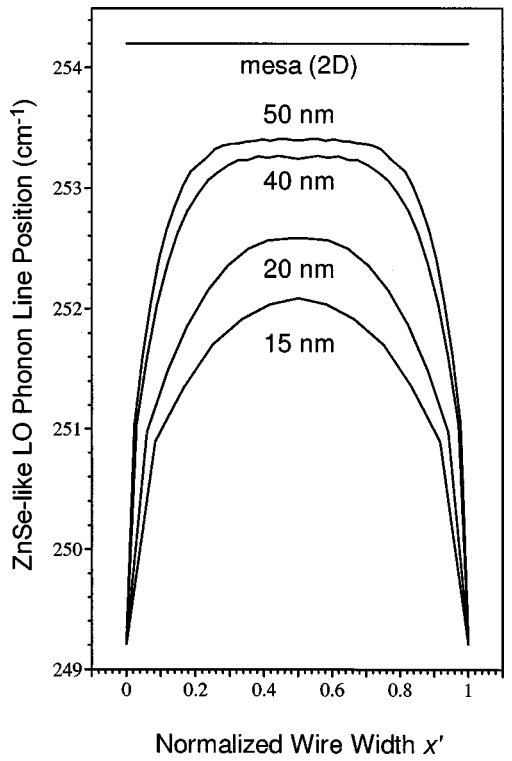

FIG. 3. Calculated LO-phonon wave-number positions of $Cd_xZn_{1-x}Se/ZnSe$ wires for different widths in the middle of the quantum-well layer as a function of the normalized coordinate x' (see Fig. 1).

with other sample areas containing wires of different width took place. Parameters that were varied in our experiments are the wire width and sample temperature. In order to separate the contribution of the substrate from that of the wires additional Raman spectra of the substrate next to the wires were taken under otherwise identical experimental conditions.

The Raman spectra taken from the $Cd_{0.35}Zn_{0.65}Se$ wires showed two peaks for low temperatures. Both were situated in the wave-number region of the ZnSe LO phonon. However, in spectra measured on the ZnSe substrate only one of these Raman bands, that at high wave numbers, could be observed. Therefore, the high-wave-number peak is assigned to the ZnSe LO from the bottom and top ZnSe layers of the quantum wire and the low-wave-number peak is the ZnSe-like LO phonon of the $Cd_{0.35}Zn_{0.65}Se$ quantum-well layer.[8] In Fig. 4 the LO-phonon wave-number positions derived from Raman spectra measured for 32-nm wires (ZnSe LO-phonon line position labeled by circles, ZnSe-like LO-phonon line position labeled by squares) and beside the wires (line positions labeled by triangles) as a function of the temperature are plotted. For 32-nm-wide wires, the splitting between the ZnSe and the ZnSe-like LO phonons in the $Cd_xZn_{1-x}Se$ layer at $T=9$ K is about 7 cm^{-1}. This wave-number splitting remains constant for increasing temperature. Due to the increasing broadening of the LO signals and the change of the resonance conditions for increasing temperature, the ZnSe-like LO-phonon line is only separable from the ZnSe LO-phonon line at temperatures lower than 150 K.

Raman spectra were also recorded as a function of the wire width. In Fig. 5 the Raman spectra of

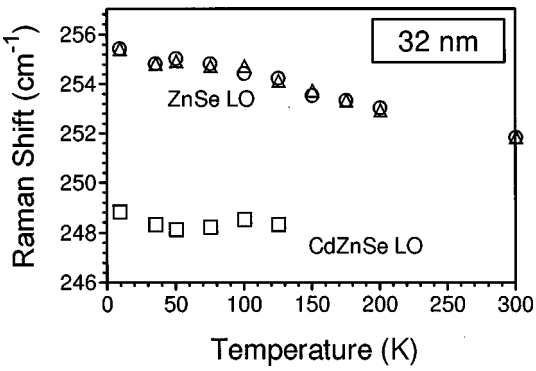

FIG. 4. Raman shift of the ZnSe LO (labeled by ○) and the ZnSe-like LO (labeled by □) phonon lines for 32-nm $Cd_{0.35}Zn_{0.65}Se/ZnSe$ wires and beside the wire regions (ZnSe LO-phonon line, labeled by △) as a function of temperature.

$Cd_{0.35}Zn_{0.65}Se/ZnSe$ wires for different widths at $T=9$ K have been plotted. It can be seen that the position of the ZnSe-like LO phonon of the $Cd_{0.35}Zn_{0.65}Se$ layer is a function of the wire width. Also, for the two-dimensional mesa the ZnSe-like LO phonon line of the $Cd_xZn_{1-x}Se$ layer is detected as a shoulder of the ZnSe LO Raman band. The splitting between the ZnSe LO-phonon line and the ZnSe like LO-phonon line of the $Cd_xZn_{1-x}Se$ layer increases for decreasing wire width. However, the Raman spectra indicate a very small wire width dependence of the ZnSe-like LO-phonon line position for wires thinner than 32 nm. The weak ZnSe TO phonon is forbidden in backscattering geometry.[20]

B. Photoluminescence

Low-temperature (2-K) PL measurements have been performed as a function of the wire width. In Fig. 6 normalized

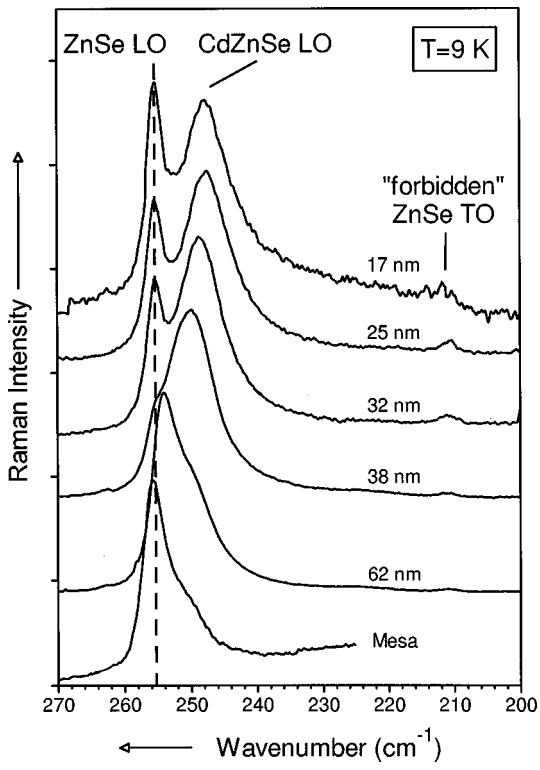

FIG. 5. Raman spectra (ZnSe LO region) of $Cd_xZn_{1-x}Se/ZnSe$ wires for different widths at $T=9$ K.

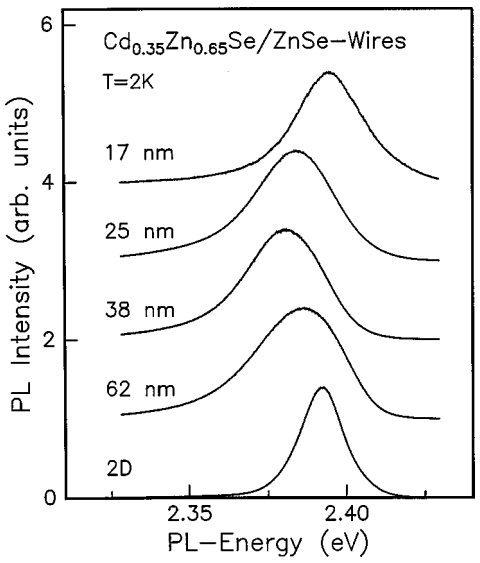

FIG. 6. Photoluminescence spectra of $Cd_{0.35}Zn_{0.65}Se/ZnSe$ wires. Spectra are shifted vertically for clarity.

PL spectra of quantum wires with different wire widths between 62 and 17 nm are compared to a 2D reference. With decreasing wire width, at first a redshift, followed by a strong blueshift for the narrowest wires, was found. To analyze the variation of the PL energy in a more detailed way, we plotted in Fig. 7 the PL energy as a function of the wire width. The PL energy of the 2D mesa signal is detected at 2.392 eV. For wire widths larger than 100 nm no substantial change of the PL energy with respect to the mesa was found. For wires in the region between 100 and 30 nm an increasing redshift for decreasing wire widths has been observed. This redshift amounts to nearly 12 meV for 30-nm wires compared with the 2D material. Because strained $Cd_xZn_{1-x}Se$ layers have a larger band gap than bulk $Cd_xZn_{1-x}Se$ (Ref. 21) a redshift in the PL energy indicates strain relaxation.

For further reduction of the wire width a continuous shift of the PL signal in the opposite direction towards higher energies is detected. In this region the smallest wires investigated with PL experiments show a PL energy of 2.400 eV which corresponds to a blueshift of 20 meV with respect to the 30-nm wires. The redshift observed in large wires in both the PL signal and the $Cd_xZn_{1-x}Se$ LO-phonon with reducing wire width is related to strain relaxation. The blueshift of the PL signal found for very narrow wires, in contrast, is due to lateral confinement effects.[5]

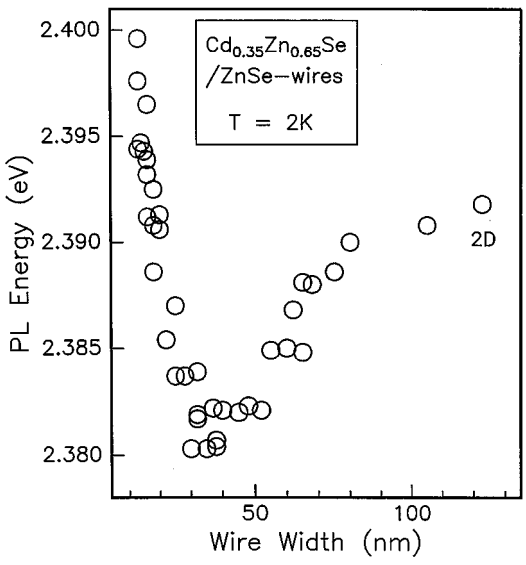

FIG. 7. Photoluminescence energy of $Cd_{0.35}Zn_{0.65}Se/ZnSe$ wires as a function of wire width.

V. DISCUSSION

In our model we assume that the wire-width-dependent Raman shift of the ZnSe-like LO phonon of the $Cd_{0.35}Zn_{0.65}Se$ layer shown in Fig. 6 is due to a change of the lattice constant caused by strain relaxation in the $Cd_{0.35}Zn_{0.65}Se$ quantum-well layer. The LO-phonon wave number of strain-free $Cd_{0.35}Zn_{0.65}Se$ bulk material[19] is about 245 cm^{-1}. The biaxial compressive strain in the epitaxial layers results in a blueshift of the ZnSe-like LO phonon (towards the ZnSe LO-phonon position).[15] To obtain quantum wires the semiconductor layer system is patterned. Therefore, at the edges of the $Cd_{0.35}Zn_{0.65}Se$ quantum wires strain relaxation occurs. This strain relaxation influences the whole $Cd_xZn_{1-x}Se$ lattice. The influence of the strain relaxation of the quantum-well layer depends on the wire width because the volume fraction of strain-relaxed $Cd_{0.35}Zn_{0.65}Se$ increases for decreasing wire width, which results in a redshift of the ZnSe-like LO phonon.[15]

The Raman spectra obtained for the different wire widths were fitted in order to obtain the exact wave-number positions of the ZnSe and ZnSe-like LO phonon. From the theoretical model we obtained the wave-number positions of the ZnSe LO phonon as well as the ZnSe-like LO phonon as a function of the coordinates of the wire cross section (see Fig. 2). From these we calculated LO-phonon shifts averaged over the wire cross section.

In Fig. 8 the differences $\Delta\tilde{\nu}$ of the LO positions of the ZnSe and ZnSe-like LO phonons of the wires relative to the position of the ZnSe LO phonon measured beside the wires have been plotted for the measurements at $T=9$ K. For a comparison also the average values obtained from the theoretical model are plotted as a function of the wire width. Figure 8 shows that for large wire widths the experimental and theoretical results are in good agreement. For small wire widths, however, the calculated splitting of the ZnSe and ZnSe-like LO phonon is smaller than the experimental value. From the theoretical model the maximum shift due to strain relaxation is expected for wire sizes smaller than 10 nm (not shown in Fig. 8). However, the experimentally observed ZnSe-like LO-phonon positions (see Fig. 8) indicate a very small wire width dependence for wires thinner than 32 nm.

In order to discuss the theoretical results in comparison with the experimental data mainly the following point has to be taken into consideration. The experimental data are observed from resonance Raman measurements. Strain and strain relaxation are responsible for nonconstant resonance conditions as a function of the wire cross-section coordinates. Therefore, the measured positions of the $Cd_{0.35}Zn_{0.65}Se$ LO phonon bands may be influenced by the resonance conditions both at the edge of a particular wire and at the middle part of this wire.

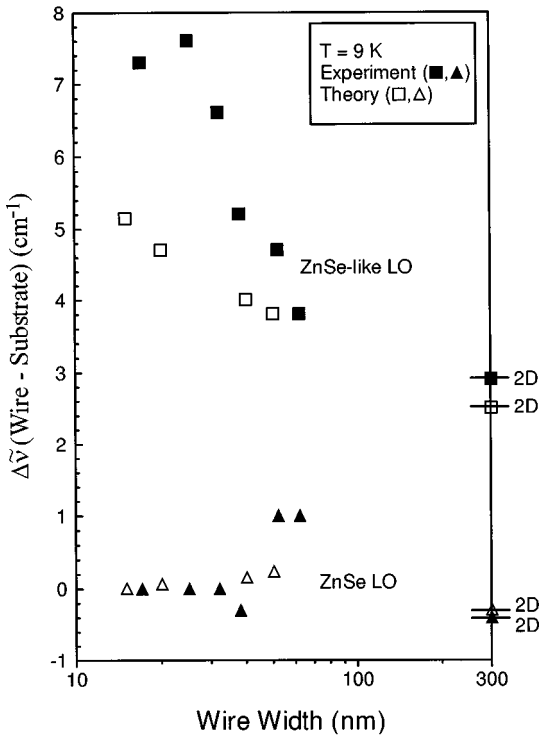

FIG. 8. Theoretical and experimental difference $\Delta\tilde{\nu}$ between the ZnSe and ZnSe-like LO-phonon line positions.

The influence of biaxial strain on the direct ($k=0$) band of zinc-blende semiconductors has been discussed in the literature.[9] Biaxially strained $Cd_xZn_{1-x}Se$ has a larger band gap than bulk $Cd_xZn_{1-x}Se$. Therefore, strain relaxation will lead to a redshift of the band-gap energy with respect to the band-gap energy of the strained layer.[17,22,23] In the case of a strain-relaxed quantum wire the band gap at the edge is smaller than the band gap in the middle of the wire. Thus the choice of the excitation wavelength determines which part of the wire is resonantly excited. As a consequence, the LO-phonon wave-number position obtained from Raman spectra cannot be simply considered as the average value of contributions arising from all parts of the wire. Rather a weighing determined by the resonance conditions has to be taken into account. With an excitation wavelength, which is in resonance with the edge of a particular wire width and only near resonance at the higher strained middle part of this wire, the LO phonon would occur in the Raman spectra at a wave-number position lower than the average value of the different ZnSe-like LO-phonon wave-number contributions calculated for this particular wire width. In this case, a change of the excitation wavelength towards higher energies would lead to a blueshift of the detected LO-phonon wave-number position.

In order to elucidate what influence such shifts of the resonance conditions have on the LO phonon line positions, we consider the temperature dependence of the Raman spectra. The band gap of a semiconductor decreases for increasing temperature. This also results in a change of the resonance conditions. For an excitation wavelength, which is only near resonance with the middle part of a particular wire width at $T=9$ K, the resonance with this middle part increases for increasing temperature. Therefore, the ZnSe-like LO-phonon position seen in the Raman spectra should be blueshifted for increasing temperature. However, this is not the case, as shown in Fig. 4. The measured splitting between the ZnSe and ZnSe-like LO remains constant for increasing temperature. Therefore, we conclude that the detected LO-phonon positions in our Raman spectra do not depend on the different resonance conditions for the edge and for the middle part of a particular wire. Further investigations concerning this problem are in progress.[24]

As discussed in Fig. 3, experiments result in a splitting between ZnSe and ZnSe-like LO phonons of about 7 cm^{-1} for wires thinner than 32 nm. Such a splitting is calculated only at the edge of the wires and the mean value calculated for the whole wire is smaller. This means that the calculated splittings are too small to explain the experimental results. Therefore, we conclude that the strain relaxation at the edge of the narrow quantum wires is larger than the theoretically predicted strain relaxation.

While Raman measurements directly probe the wire width dependence of the LO-phonon energy, the PL experiments yield information about the size-dependent variation of the band gap. As discussed above, a biaxially strained $Cd_xZn_{1-x}Se$ layer is characterized by a larger band gap compared to unstrained bulk material. Thus the strain relaxation in deep etched wires, which is indicated by the Raman data, should result in a redshift of the band gap with decreasing wire size. From these considerations, the size-dependent redshift of the PL signal down to wire widths of about 30 nm (see Fig. 7) can be understood easily.

However, the strong blueshift for wires below 30 nm is not a strain effect, but occurs due to lateral quantization effects that must be considered for wires of these sizes, as reported elsewhere.[5,6] The contribution of the lateral confinement can be estimated by a simple model using a square-well potential. Apparently, the quantization effects dominate for the narrow wires because for the description of the PL data strain effects can be neglected to achieve good agreement between the model and experiment. This implies that the strain contribution on the PL energy for these extremely narrow wires is nearly constant. This is in agreement with the data obtained by Raman measurements, where the experimentally observed ZnSe-like LO-phonon wave-number positions (see Figs. 5 and 8) also show a rather small wire width dependence for wires smaller than 32 nm.

We want to emphasize that PL and micro resonance Raman experiments lead to similar results. In both cases a strong influence of the gradual strain release is found for wire sizes between 100 and 30 nm. The redshift of the PL energy observed for wires wider than 30 nm as well as the wire-width-dependent ZnSe-like LO phonon results from the increasing role of strain relaxation for decreasing wire widths. Having in mind the simplicity of the model applied for the calculations, our theoretical results describe the experimental data fairly well. For wires below 30 nm the experiments give no indication for a significant further strain relaxation of the as-etched wire structures.

VI. CONCLUSION

In conclusion, $Cd_xZn_{1-x}Se$/ZnSe quantum wires were studied by means of micro-Raman spectroscopy and photo-

luminescence measurements. The experimental data are characterized by three different size regimes. For very wide wires (i.e., $L_x > 100$ nm), the wire data are comparable to the 2D reference. An increase of the band gap as well as an increase of the ZnSe-like LO-phonon energy compared to the unstrained $Cd_xZn_{1-x}Se$ bulk material is observed in the biaxially strained $Cd_xZn_{1-x}Se$ layers. Reduction of the wire size down to about 30 nm leads to a size-dependent strain relaxation. This is indicated by both the decrease of the band gap and the reduction of the LO-phonon energy of the ZnSe-like phonon in the wire. In order to discuss the Raman data more quantitatively, detailed calculations of the lateral strain distribution in the wires and the strain-induced change of the LO-phonon energy were performed. For large wires, reasonable agreement between the experimental data and the theory is obtained. This demonstrates the necessity to take into account the strain release in quantum wires in order to understand Raman as well as PL data. Reducing further the lateral sizes of the wires below 30 nm, the splitting between the ZnSe LO phonon of the barrier and the ZnSe-like phonon of the $Cd_xZn_{1-x}Se$ remains nearly constant, indicating that no significant further strain release occurs in narrow wires. While the discrepancy between Raman data and theory in this size regime is not fully understood yet, the experimental data are in good agreement with the PL measurements: For wires smaller than 30 nm, a distinct blueshift of the PL signal is observed with decreasing wire size. This blueshift can be explained easily by taking into account lateral confinement effects, while the variation of the band gap due to strain relaxation seems to be negligible in this size regime.

ACKNOWLEDGMENTS

We gratefully acknowledge financial support from the Deutsche Forschungsgemeinnschaft (Sonderforschungsbereich 410, Teilprojekte Al, C1, and C3). G. Le., T.B., A.M., and W.K. also acknowledge support from the Fonds der Chemischen Industrie. We wish to thank B. Jobst and D. Hommel, Experimentelle Physik III, for providing the MBE grown samples.

*Author to whom correspondence should be addressed.

[1] W. Walecki, W. Patterson, A. V. Nurmikko, H. Lou, N. Samarth, J. Furdyna, M. Kobayashi, S. Durbin, and R. Gunshor, Appl. Phys. Lett. **57**, 2641 (1990).

[2] J. Ding, A. V. Nurmikko, D. C. Grillo, L. He, and R. Gunshor, Appl. Phys. Lett. **63**, 2255 (1993).

[3] L. S. Dang, C. Gourgon, N. Magnea, H. Mariette, and C. Vieu, Semicond. Sci. Technol. **9**, 1953 (1994).

[4] C. M. Sotomayor Torres, A. P. Smart, M. Watt, M. A. Foad, K. Tsutsui, and C. D. W. Wilkinson, J. Electron. Mater. **23**, 289 (1994).

[5] M. Illing, G. Bacher, T. Kümmell, A. Forchel, T. G. Andersson, D. Hommel, B. Jobst, and G. Landwehr, Appl. Phys. Lett. **67**, 124 (1995).

[6] M. Illing, G. Bacher, T. Kümmell, A. Forchel, D. Hommel, B. Jobst, and G. Landwehr, J. Vac. Sci. Technol. B **13**, 2792 (1995).

[7] C. M. Sotomayor Torres, A. Ross, Y. S. Tang, A. Ribayrol; S. Thoms, A. S. Bunting, H. P. Zhou, K. Tsutsui, H. McLelland, H. P. Wagner, B. Lunn, and D. E. Ashenford (unpublished).

[8] G. Lermann, T. Bischof, A. Materny, W. Kiefer, T. Kümmell, G. Bacher, A. Forchel, and G. Landwehr, J. Appl. Phys. **81**, 1446 (1997).

[9] B. Rockwell, H. R. Chandrasekhar, M. Chandrasekhar, A. K. Ramdas, M. Kobayashi, and R. L. Gunshor, Phys. Rev. B **44**, 11 307 (1991).

[10] Physics of II-VI and I-VII Compounds, Semimagnetic Semiconductors, edited by O. Madelung, Landolt-Börnstein, New Series, Group III, Vol. 17, pt. b (Springer, Berlin, 1982).

[11] M. Lankers, D. Göttges, A. Materny, K. Schaschek, and W. Kiefer, Appl. Spectrosc. **46**, 1331 (1992).

[12] V. Deckert and W. Kiefer, Appl. Spectrosc. **46**, 322 (1992).

[13] E. Anastassakis, in *Proceedings of the Sat. Symposium on European Solid State Device Research Conference, Berlin, 1989*, edited by A. Heuberger (The Electrochemical Society, New York, 1989), Vol. 90-11, p. 298.

[14] F. Cerdeira, C. J. Buchenauer, F. H. Pollak, and M. Cardona, Phys. Rev. B **5**, 580 (1972).

[15] S. Nakashima, A. Fujii, K. Mizoguchi, A. Mitsuishi, and K. Yoneda, Jpn. J. Appl. Phys., Part 1 **27**, 1327 (1988).

[16] S. C. Jain, B. Dietrich, H. Richter, A. Atkinson, and A. H. Harker, Phys. Rev. B **52**, 6247 (1995).

[17] I. Tan, R. Mirin, T. Yasuda, E. L. Hu, J. Browers, C. B. Prater, P. K. Hansma, M. Y. He, and A. G. Evans, J. Vac. Sci. Technol. B **10**, 1971 (1992).

[18] M. Notomi, J. Hammersberg, H. Wemau, S. Nojima, H. Sugiura, M. Okamoto, T. Tamamura, and M. Potemski, Phys. Rev. B **52**, 11 147 (1995).

[19] R. G. Alonso, E.-K. Suh, A. K. Ramdas, N. Samarth, H. Luo, and J. K. Furdyna, Phys. Rev. B **40**, 3720 (1989).

[20] B. Jusserand and M. Cardona, in *Light Scattering in Solids V*, edited by M. Cardona and G. Güntherodt (Springer-Verlag, Berlin, 1989), p. 49.

[21] H. J. Lozykowski and V. K. Shastri, J. Appl. Phys. **69**, 3235 (1991).

[22] H. Straub, G. Brunnthaler, W. Faschinger, G. Bauer, and C. Vieu, J. Cryst. Growth **159**, 451 (1996).

[23] R. Steffen, A. Forchel, T. L. Reinecke, T. Koch, M. Albrecht, J. Oshinowo, and F. Faller, Phys. Rev. B **54**, 1510 (1996).

[24] G. Lermann, T. Bischof, B. Schreder, A. Materny, W. Kiefer, T. Kümmell, G. Bacher, A. Forchel, and G. Landwehr (unpublished).